**ORIGINAL ARTICLE**

# MR imaging characterization of pheochromocytoma: a comparison between typical and atypical tumor lesions

Simone Maurea[1] · Ludovica Attanasio[1] · Roberta Galatola[1] · Valeria Romeo[1] · Arnaldo Stanzione[1] · Luigi Camera[1] · Michele Klain[1] · Chiara Simeoli[2] · Roberta Modica[2] · Massimo Mascolo[1] · Giovanni Aprea[3] · Mario Musella[1] · Arturo Brunetti[1]

## Abstract

**Purpose** The aim of this retrospective study was to compare the MRI features between typical and atypical pheochromocytomas (Pheos) to specifically illustrate MRI features of atypical tumors for helping tumor diagnosis.

**Methods** A total of 22 patients (14 women and 8 men, median age: 53 years, age range: 25–82 years) with Pheos evaluated using a 3 T MRI scanner were retrospectively collected; in particular, all patients had one tumor lesion, except in two cases who had two and three lesions, respectively, for a total of 25 tumor lesions.

**Results** Of the total 25 tumor lesions included in our series, 12 lesions were classified as typical for their classical appearance on MRI (T1 hypointensity, T2 hyperintensity, no signal drop on T1 out-of-phase, restricted diffusion and persistent contrast enhancement). Conversely, the other 13 tumors were classified as having atypical lesions because they did not show the MRI features observed in typical Pheos; in particular, 3 lesions showed signal intensity suggestive of tumor hemorrhagic changes, 2 lesions were totally cystic with an internal fluid–fluid level and a thin capsula, 3 lesions showed predominantly cystic signal intensity with residual solid tissue in the peripheral capsula, and the remaining 5 lesions appeared as rounded partially cystic lesions with associated areas of solid tissue.

**Conclusion** The imaging characterization of typical Pheos may be performed using MRI with specific imaging features; however, atypical Pheos represents a diagnostic challenge using MRI; in these tumors, cystic, necrotic, hemorrhagic, or fat changes may occur; thus, diagnostic pitfalls should be taken into consideration for MRI interpretation of such tumor type in clinical practice.

**Keywords** Pheochromocytoma · MRI · Characterization · Typical · Atypical

## Introduction

Pheochromocytomas (Pheos) are usually functional tumors of adrenal medulla chromaffin tissue [1]; hence, Pheos are commonly symptomatic for increasing catecholamine plasma and urinary levels; therefore, imaging evaluation is performed for lesion detection and successively to establish treatment options [2, 3]. In this regard, magnetic resonance imaging (MRI) and computed tomography (CT) are the imaging techniques of choice for scanning the superior abdomen. In particular, MRI provides specific imaging criteria to characterize Pheo; usually, as typical forms, Pheos appear as solid round masses of variable size with homogeneous increased signal intensity on T2-weighted and low signal intensity on T1-weighted images with clear enhancing and poor washout after contrast administration on T1-weighted dynamic contrast-enhanced (DCE) sequence [2, 4]. However, Pheos may have atypical imaging appearance when different types of lesion degeneration such as necrosis, hemorrhage, calcification, and cystic or intracellular lipid changes may occur; of note, in these atypical forms, the differential

✉ Arnaldo Stanzione
arnaldo.stanzione@unina.it

1 Department of Advanced Biomedical Sciences, University of Naples "Federico II", Via S. Pansini, 5, 80123 Naples, Italy

2 Department of Clinical Medicine and Surgery, Division of Endocrinology, University of Naples "Federico II", Naples, Italy

3 Department of General and Mini-invasive Surgery, University of Naples "Federico II", Naples, Italy

diagnosis with other adrenal tumors may be difficult [2, 5, 6]. In detail, Jacques et al. [5] reported increased MRI signal intensity heterogeneity correlating pathologically with high amounts of hemorrhage, necrosis, and fibrosis; of note, cystic degeneration may be so wide that only a small amount of viable cells may remain to identify the true nature of lesion [7]; different atypical types of Pheos such as cystic, hemorrhagic, calcific, and adipose have been reported. Thus, the diagnosis of these atypical Pheos is not clinically easy, specifically when adrenal function is normal, with delayed patient management [1, 8]. Furthermore, Pheos can present as adrenal incidentalomas, and they can occasionally be non-functioning, conditions in which the diagnosis can prove more complex [9, 10].

The aim of this retrospective study was to compare the MRI features between typical and atypical Pheos to specifically illustrate MRI features of atypical tumors for helping tumor diagnosis in clinical practice.

## Materials and methods

### Study population

This retrospective study had regular approval by our institutional review board (protocol code: 10/17), and informed patient consent was obtained in all cases. Our institutional archive was searched to identify abdominal MRI scans of patients with adrenal lesions detected by previous ultrasound and/or computed tomography scans in the period from 2008 to 2023; radionuclide imaging studies were also collected and reviewed when available. Patients with Pheos were extracted and included in the final study population using the following criteria: (1) Pheo diagnosis proven by histopathology or confirmed by radionuclide studies ($[^{131}I]/$ $[^{123}I]$ metaiodobenzylguanidine—MIBG); (2) pre-treatment MRI study available; and (3) clinical and laboratory data related to adrenal pathology retrievable from medical records. MRI scans with significant artifacts were excluded.

### MRI protocol

A 3 T device (Magnetom Trio, Siemens, Erlangen, Germany) with a surface–body coil was used to perform MRI studies. Imaging procedure included pre- and post-contrast sequences: CS T1 VIBE (TR/TE = 4.04/1.26 ms; TR/TE = 4.04/2.59; slice thickness = 3 mm; no gap) in- and out-of-phase on axial planes, T2 HASTE (TR/TE = 2000/90 ms; slice thickness = 3 mm; gap = 0.6 mm) with fat suppression on axial planes, T2 HASTE (TR/TE = 2000/90 ms; slice thickness = 3 mm; gap = 0.6 mm) on axial and coronal planes, and axial diffusion-weighted imaging (DWI) using an "echoplanar imaging single shot" (SS-EPI) sequence with fat suppression and integrated

parallel imaging (GRAPPA-2) (TR = 5700 ms, TE = 69 ms, slice thickness = 4 mm; matrix size = 128 Å ~ 128; averages = 5; *b*-value = 50, 500, and 1000 s/mm, acquisition time = 3.07 min); an ADC map was computed using a monoexponential model on the imaging console (Syngo VE 36 A, Siemens, Erlangen, Germany). DCE (0.1 mmol/kg Gd-DTPA Magnevist, Bayer Pharma, Berlin, Germany) T1 VIBE 3D (TR/TE = 3.3/1.1 ms; slice thickness = 2 mm; no gap) sequence was performed in arterial (30 s), portal (60 s), and delayed phases (5 min) on axial planes after injection.

### Imaging analysis

MRI studies were evaluated by two radiologists expert in abdominal imaging working in consensus to detect adrenal tumors as well as to describe lesion structure, characteristics, and size according to MR images. They were blinded to clinical and histopathological data. The MR images were anonymized and evaluated in a random order. In particular, all sequences of the same MRI study were contextually visualized to qualitatively assess tumor lesion signal intensity on T1, T1 CS, T2, and T1 DCE images; a 3-point scoring (0 = hypointensity compared to the liver, 1 = isointensity compared to the liver, and 2 = hyperintensity compared to the liver) was used to qualitatively assess tumor lesion signal intensity. Pheos were classified into two groups based on their typical or atypical features on MRI, as previously described [6]; typical Pheos consisted of a homogeneous solid mass with low T1 signal intensity, high T2 signal intensity, no signal drop on T1 out-of-phase CS sequence, and clearly enhancing and poor washout on T1 FS DCE sequence. On the contrary, atypical Pheos consisted of cystic, hemorrhagic, calcific, and adipose types; of note, cystic changes were total, predominant, or partial, as previously described [6].

### Statistical analysis

Data extracted from medical records and MR images were organized in a digital spreadsheet, which was also used to perform descriptive statistics calculations. In particular, numeric variables were presented as mean ± standard deviation of median and range as appropriate, while categorical variables as count and percentage (Excel 2020, Microsoft, Washington, WA, USA).

## Results

### Study population

A total of 22 patients, of which 14 (64%) were female with a median age of 53 years (age range: 25–82 years), with Pheos

were evaluated. In particular, since 2 patients had multiple lesions (i.e., 2 and 3, respectively), 25 Pheos were included. Half of the patients (11/22, 50%) were symptomatic, with the most commonly encountered clinical symptom being high blood pressure (9/11, 82%), while tachycardia and recurrent headache with night sweats were encountered in a single patient each. Final histopathology confirmation was available for 22/25 (88%) adrenal lesions; for the remaining cases, MIBG exams were used to confirm Pheos diagnosis [8]. Laboratory evaluation of adrenal medullary function showed hypersecretion in 12/22 (55%) patients. No MRI scan was excluded due to the presence of artifacts.

### Imaging analysis

After image evaluation, 12/25 (48%) lesions in 10/22 (45%) patients were classified as typical according to MRI features (Table 1). The imaging example of a typical Pheo is shown in Fig. 1. Conversely, the other 12/22 (55%) patients presented 13/25 (52%) lesions classified as atypical Pheos due to the lack of typical Pheos features (Table 2). In particular, 3/13 (23%) lesions showed areas of high signal intensity on T1 images, suggesting hemorrhagic changes. The remaining lesions (9/13, 77%) were either totally (2/13, 15%), predominantly (3/13, 23%), or partially (5/13, 39%) cystic, with two of the latter lesions showing fat inclusions (both from the same patient). Final diagnosis was confirmed by MIBG in one atypical and two typical Pheos, while all the remaining lesions were determined on histopathologic evaluation. The

imaging examples of hemorrhagic, totally, predominantly, and partially cystic atypical Pheos are shown in Figs. 2, 3, 4, and 5, respectively.

## Discussion

Pheos are catecholamine-secreting tumors arising in the chromaffin cells of adrenal medulla [1–3]. The majority (90%) of Pheos are located within the adrenal glands, while extra-adrenal Pheos develop in paraganglionic chromaffin tissue of the sympathetic nervous system; these lesions may occur anywhere from the base of the brain to the urinary bladder and are named paragangliomas. Accurate pre-surgical diagnosis is really important because untreated Pheos may determine clinically significant cardiac arrhythmias and hypertension with potential fatal clinical events. Of note, patients may be also completely asymptomatic, with up to 10% of cases being clinically silent; despite their usual unilateral and benign appearance, Pheos can be bilateral and malignant in 10% of cases.

Tumor diagnosis depends on imaging detection of an adrenal lesion associated with specific clinical symptoms and laboratory demonstration of increased catecholamine secretion. Usually, on CT, Pheos show specific imaging features as solid, hypervascular tumors with increased CT density (> 10 UH); rarely do they contain sufficient intracellular fat to have an attenuation of less than 10 HU [2]. The common MRI appearance of typical Pheos is a mass with

**Table 1** MRI characteristics of typical pheochromocytomas

| # | Patient | | MRI structure | Tumor size (mm) | MRI sequences[a] | | | | | | | |
|---|---|---|---|---|---|---|---|---|---|---|---|---|
| | Sex | Age (years) | | | T1 CS IP | T1 CS OP | T2 | T2 FS | DWI | ADC | Pre-CE T1 FS | Post-CE T1 FS |
| #1 | F | 82 | Solid | 23 | 0 | 0 | 2 | 2 | 2 | 0 | 0 | 2 |
| #2 | M | 72 | Solid heterogeneous | 38 | 0 | 0 | 2 | 2 | na | na | 0 | 2 |
| #3 | M | 25 | Solid | 80 | 0 | 0 | 2 | 2 | na | na | 0 | 2 |
| #4 | F | 73 | Solid | 15 | 0 | 0 | 2 | 2 | 2 | 0 | 0 | 2 |
| #5 | F | 32 | Solid | 48 | 0 | 0 | 2 | 2 | na | na | na | na |
| #6 | M | 56 | Solid | 50 | 0 | 0 | 2 | 2 | na | na | 0 | 2 |
| #7 | M | 58 | Solid heterogeneous | 29 | 0 | 0 | 2 | 2 | na | na | 0 | 2 |
| #8 a | M | 42 | Solid (right) | 9 | 0 | 0 | 2 | 2 | na | na | 0 | 2 |
| #8 b | | | Solid (right) | 20 | 0 | 0 | 2 | 2 | na | na | 0 | 2 |
| #8 c | | | Solid (left) | 50 | 0 | 0 | 2 | 2 | na | na | 0 | 2 |
| #9 | F | 57 | Solid heterogeneous | 30 | 0 | 0 | 2 | 2 | na | na | 0 | 2 |
| #10 | F | 42 | Solid | 18 | 0 | 0 | 2 | 2 | 2 | 0 | 0 | 2 |

Patient #8 had tumor lesions

*CS* chemical shift, *IP* in phase, *OP* out phase, *FS* fat suppressed, *CE* contrast enhanced, *na* not available

[a]A 3-point scoring (0 = hypointensity compared to the liver, 1 = isointensity compared to the liver, and 2 = hyperintensity compared to the liver) was used to qualitatively assess tumor lesion signal intensity*CS*
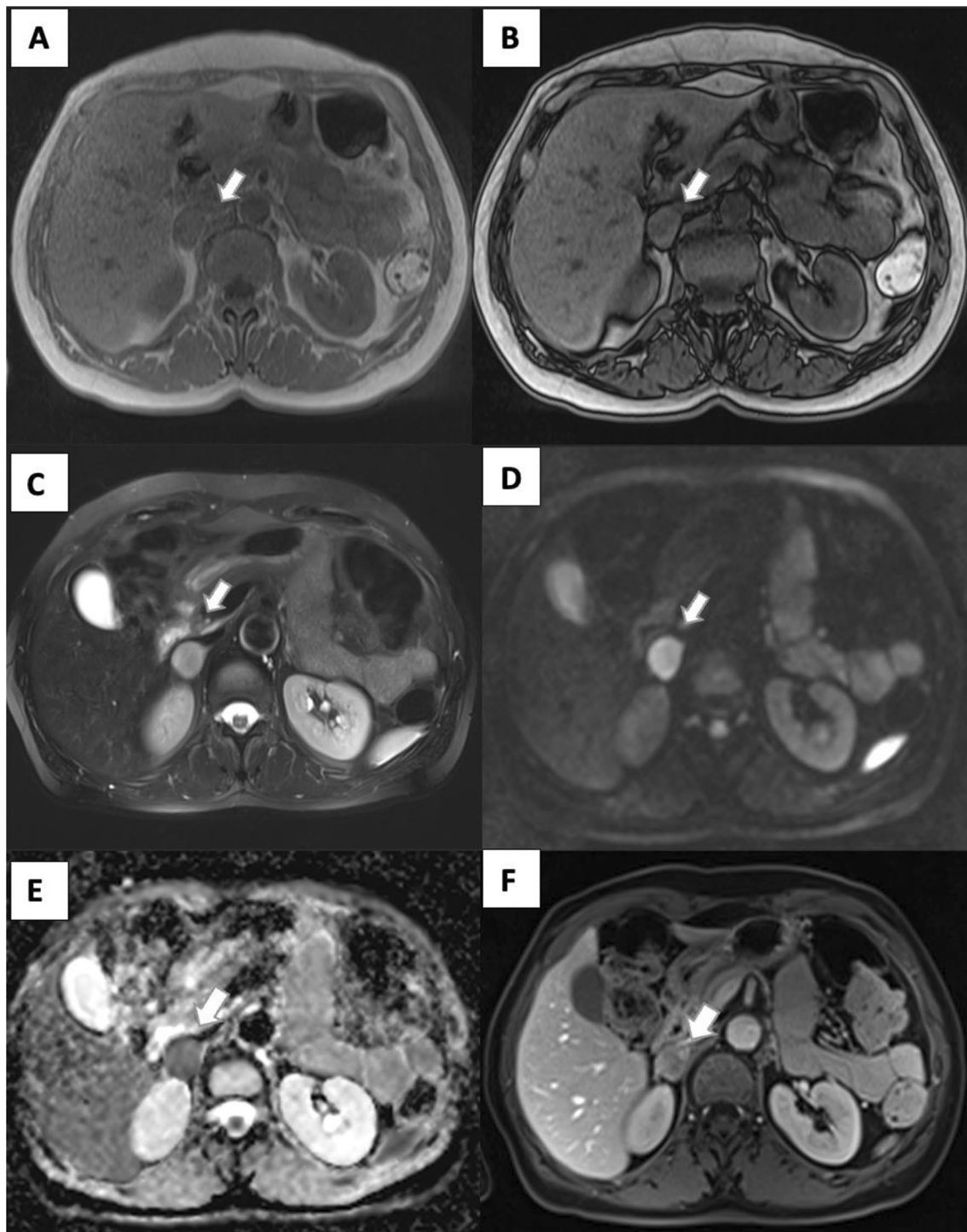
**Fig. 1** Typical medium-sized (23 mm) left adrenal Pheo (#1, Table 1). A homogeneous left adrenal mass with regular margins and signal hyperintensity was detected on fat suppression (FS) low signal intensity on T1 sequence and high signal intensity on T2 sequence; furthermore, Pheos commonly enhance avidly on T1 imaging after administration of a gadolinium-based contrast material [2]. Radionuclide techniques may T2-weighted MRI (**A**); the lesion had no change on T1-weighted out-of-phase (**B**), showed restricted diffusion (**C**, **D**) and persistent contrast enhanced on FS T1-weighted delayed image (**E**)

low signal intensity on T1 sequence and high signal intensity on T2 sequence; furthermore, Pheos commonly enhance avidly on T1 imaging after administration of a gadolinium-based contrast material [2]. Radionuclide techniques may also be used to characterize Pheos using specific radiocompounds such as MIBG and/or labeled somatostatin analogs [11–13]. However, Pheos may be incorrectly categorized as adenomas showing fat inclusions or may undergo a variety

**Table 2** B MRI characteristics of atypical pheochromocytomas

| # | Patient | | MRI | Tumor | MRI sequences[a] | | | | | | | |
|---|---|---|---|---|---|---|---|---|---|---|---|---|
| | Sex | Age (years) | structure | size (mm) | T1 CS IP | T1 CS OP | T2 | T2 FS | DWI | ADC | Pre-CE T1 FS | Post-CE T1 FS |
| #1 | M | 67 | Hemorrhagic degeneration | 25 | 1/2° | 1/2° | 1/2° | 1/2° | 1/2° | 1/2° | 1/2° | 1/2° |
| #2 | F | 54 | Predominantly cystic | 44 | 0/1° | 0/1° | 2 | 2 | 2 | 0/2° | 0/1° | 0/2° |
| #3 | M | 34 | Predominantly cystic | 57 | 0/1° | 0/1° | 2 | 2 | na | na | 0/1° | 0/2° |
| #4 | F | 41 | Totally cystic | 50 | 0 | 0 | 2 | 2 | 2 | 2 | 0 | 0 |
| #5 | F | 72 | Totally cystic | 70 | 0 | 0 | 2 | 2 | 2 | 2 | 0 | 0 |
| #6 | F | 61 | Hemorrhagic degeneration | 38 | 0/2° | 0/2° | 1/2° | 1/2° | na | na | 0/2° | 1/2° |
| #7 | M | 57 | Predominantly cystic | 47 | 0 | 0 | 2 | 2 | 2 | 2 | 0 | 0/2° |
| #8 | F | 42 | Partially cystic | 50 | 1 | 1 | 1/2° | 1/2° | 2 | 0/2° | 1 | 1/2° |
| #9 | F | 30 | Partially cystic | 40 | 1 | 1 | 1/2° | 1/2° | na | na | 1 | 1/2° |
| #10 | F | 71 | Hemorrhagic degeneration | 95 | 0/2° | 0/2° | 1/2° | 1/2° | 2° | 0° | 0/2° | 0/2° |
| #11 | F | 58 | Partially cystic | 48 | 0/1° | 0/1° | 1/2° | 1/2° | 2 | 0/2° | na | na |
| #12a | F | 52 | Partially cystic with fat inclusions | 30 (rg) | 0/1° | 0/1° | 2° | 2° | 2° | 0° | 0/1° | 1/2° |
| #12b | | | (bilateral) | 30 (lf) | 1/2° | 1/0° | 2° | 2° | 2° | 2° | 1/2° | 0/2° |

Patient #12 had bilateral tumor

CS chemical shift, IP in phase, OP out phase, FS fat suppressed, CE contrast enhanced, ° inhomogeneous, na not available, rg right, lf left

[a]A 3-point scoring (0 = hypointensity compared to the liver, 1 = isointensity compared to the liver, and 2 = hyperintensity compared to the liver) was used to qualitatively assess tumor lesion signal intensity
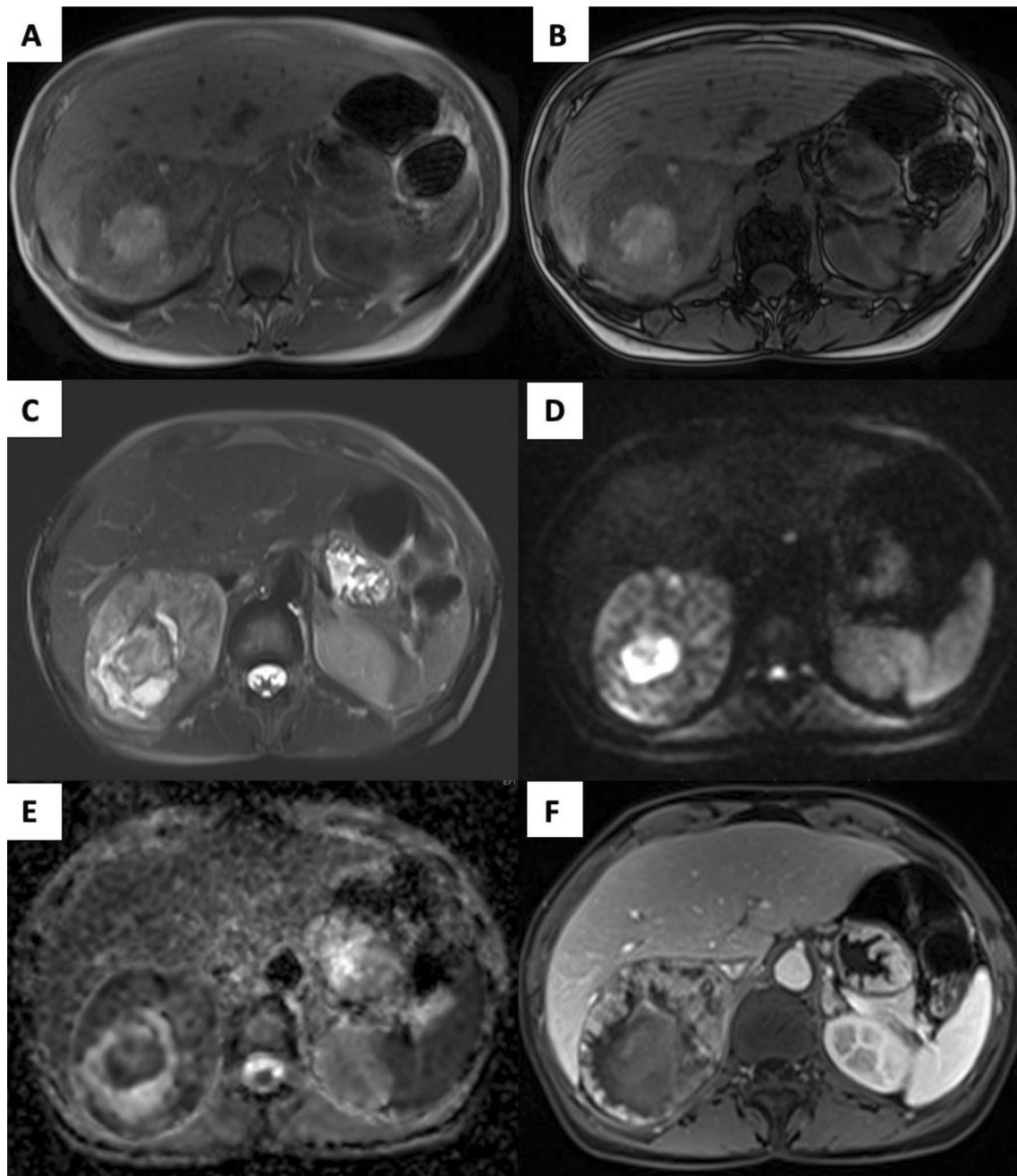
**Fig. 2** Atypical large-sized (95 mm) hemorrhagic left adrenal Pheo (#10, Table 2). An inhomogeneous large left adrenal mass with regular margins and partial signal hyperintensity was detected on T1-weighted in-phase (**A**) reflecting intralesion bleeding; the lesion had no change on T1-weighted out-of-phase (**B**), showed inhomogeneous restricted diffusion (**C**, **D**) and enhancement on FS T1-weighted delayed image (**E**)

of tissue degeneration, such as tumor hemorrhage or lesion cystic degeneration (total, predominant, or partial), which compromises their typical imaging features; these changes reflect the "chameleon" epithet given to this tumor in its atypical appearance [5–8]. In particular, these atypical Pheos may be misdiagnosed since they occur more frequently in asymptomatic patients without biochemical abnormalities compared to typical solid tumors [8]. Of note, to avoid this misdiagnosis, MRI signal intensity heterogeneity has been reported, reflecting tumor changes in atypical Pheos [5]. Recently, MRI has been confirmed to be necessary to rule out Pheo diagnosis in the case of adrenal masses with HU more than 10 [14]. However, MRI signal intensity heterogeneity may also occur in other adrenal masses of different
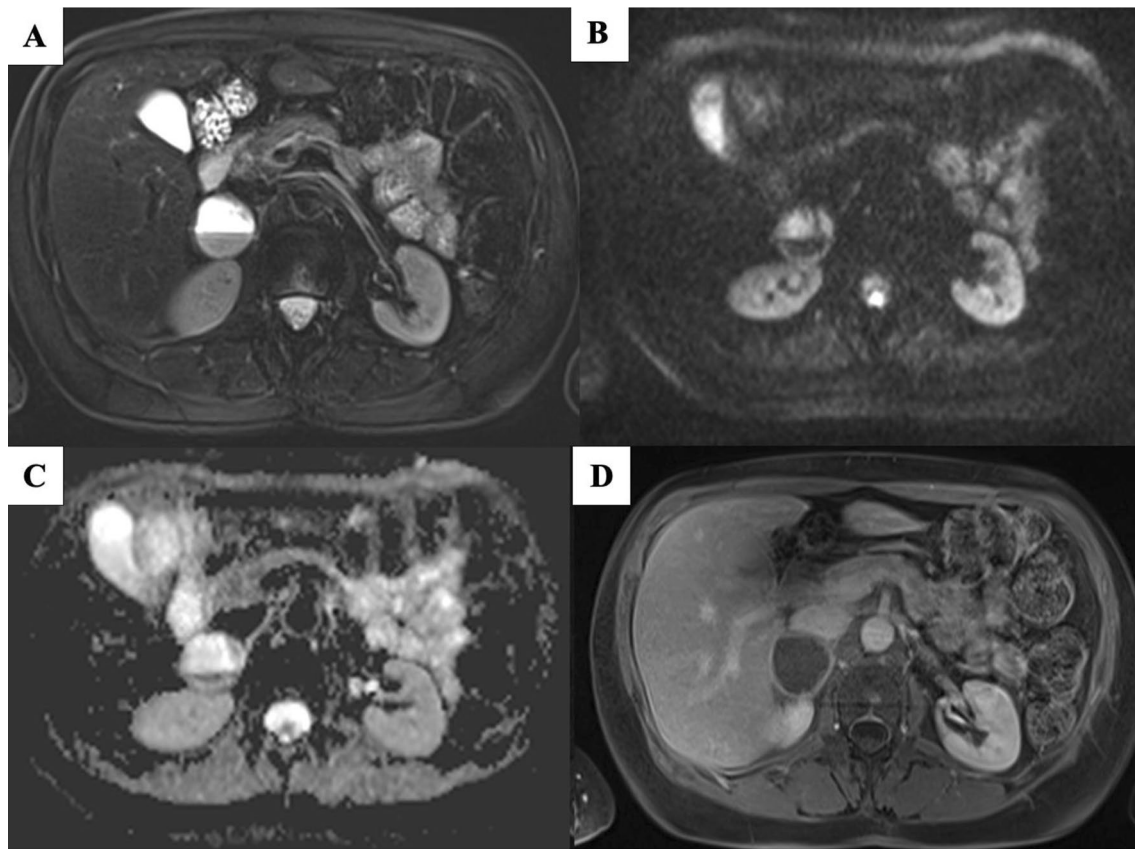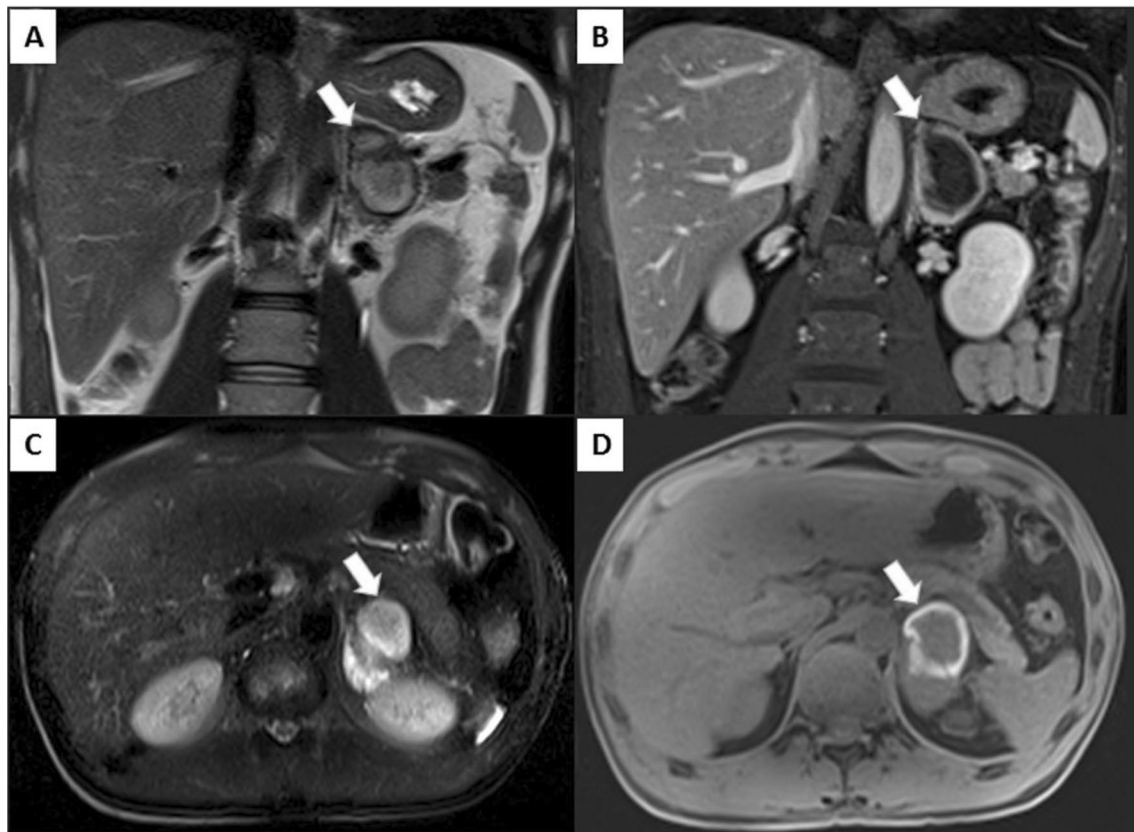
**Fig. 3** Atypical totally cystic Pheo measuring 50 mm (#4, Table 2). An inhomogeneous, well-capsulated, round adrenal mass with partial signal hyperintensity and intratumor linear level was detected on axial T2-weighted fat-suppressed image (**A**); the lesion had no restricted diffusion (**B**, **C**) and showed only capsular enhancement on FS T1-weighted delayed image (**D**)

nature [15]; thus, the detection of atypical Pheos represents a diagnostic challenge using MRI. Furthermore, although quantitative evaluation has been proposed in adrenal imaging for lesion characterization [16], this approach shows wide limitations in the case of large heterogeneous adrenal lesions [17]. Furthermore, radiomics imaging studies using CT and FDG PET/CT have been reported to characterize Pheos [18, 19].

In this study, we evaluated the MRI features to characterize typical or atypical Pheos by systematically comparing imaging appearance of these tumors. In our experience, an interesting imaging finding was that the majority (54%) of patients with Pheos had atypical lesions. In detail, we observed 12 solid tumor lesions classified as typical, while the other 13 tumor lesions showed unusual MRI features and were classified as atypical. The majority (67%) of typical Pheos (8/12) showed homogeneous hyperintensity on T2 images, while the remaining 4 lesions showed bright signal intensity, isointense to the cerebrospinal fluid (CSF), on T2 images, confirming the low occurrence (33%) of the CSF lightbulb bright signal intensity as previously reported in the literature [5, 7]. All the typical Pheos showed no signal loss on T1 out-of-phase CS sequence and significant contrast enhancement on T1 FS post-contrast DCE sequence. Conversely, the majority (77%) of atypical Pheos (10/13) were cystic, suggesting that cystic changes represent the most frequent tissue degeneration in such lesions. Of note, five of these tumors were totally or predominantly cystic surrounded by a residual viable tissue in the peripheral capsule or the remnant solid component, respectively; only five lesions appeared as partially cystic with contextual areas of solid tissue or fat inclusions. The remaining three atypical Pheos showed areas of high signal intensity on T1 images, suggesting hemorrhagic degeneration. The majority (92%) of atypical Pheos showed no signal loss on T1 out-of-phase CS sequence, confirming that the presence of intracytoplasmic lipid content is rare, as well as showed heterogeneous enhancement on T1 FS post-contrast DCE sequence according to degrees of degeneration. Therefore, the results of our experience show that atypical Pheos may be frequent and there are no specific criteria to correctly identify such tumor lesions since cystic or hemorrhagic degeneration may also occur in other adrenal tumors [20, 21]. Finally, we wish to underline that while a few case reports on atypical Pheos

**Fig. 4** Atypical predominantly cystic Pheo measuring 57 mm (#3, Table 2). An inhomogeneous, well–capsulated, round adrenal mass with signal hyperintensity was detected on coronal T2-weighted image (**A**, white arrow); the lesion was predominantly cystic on coronal FS T1-weighted image (**B**, white arrow); of note, the lesion had a hemorrhagic rim as detected on axial fat-suppressed T2-weighted image (**C**, white arrow) and axial fat-suppressed T1-weighted pre-contrast image (**D**, white arrow)
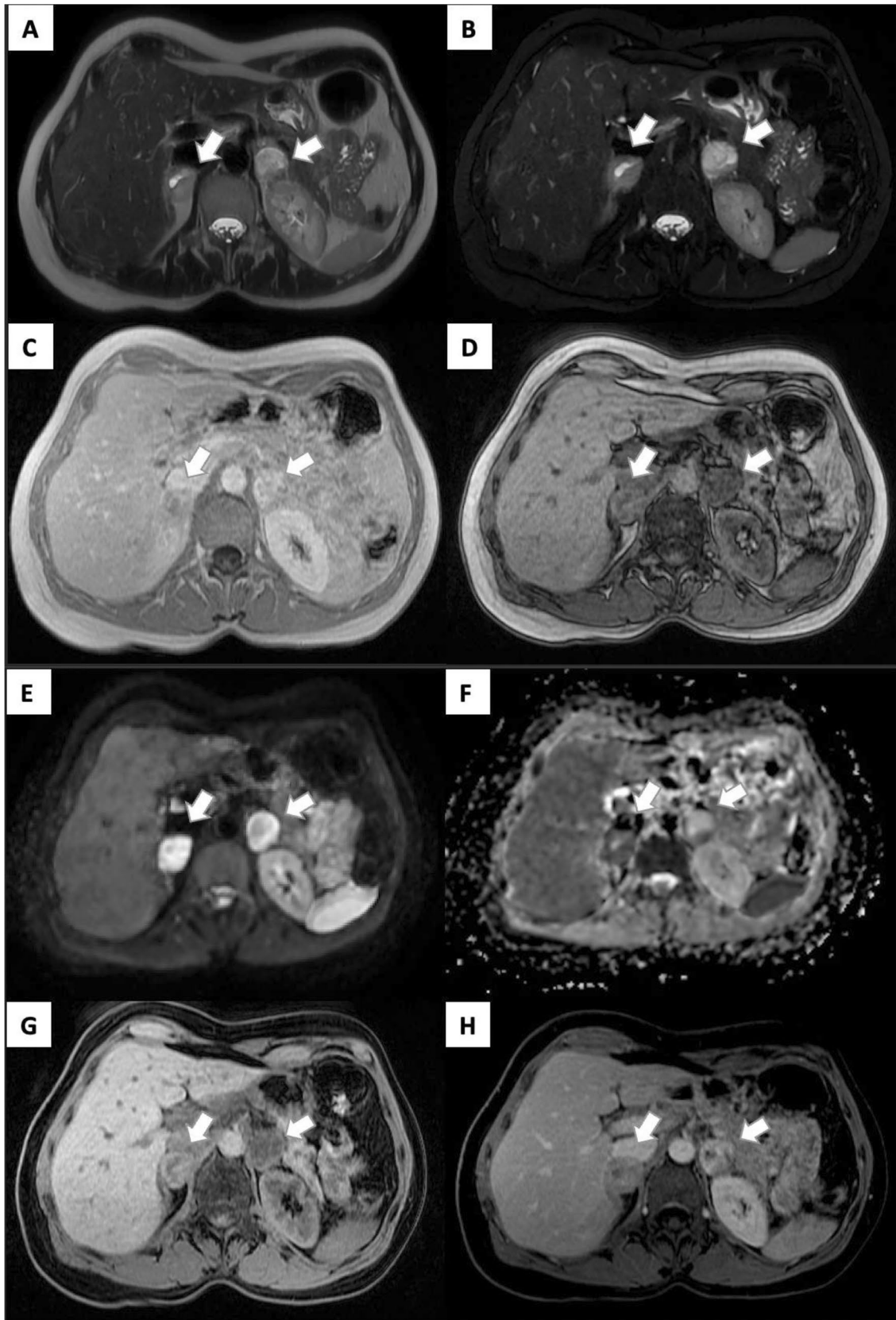
have been published in recent years, there is an overall scarcity of publications dealing with MRI features and providing multiple cases [22, 23].

Our study has some limitations that deserve to be acknowledged. First, the retrospective design and wide temporal range of data collection expose to a risk of selection bias, which probably explains why the number of atypical Pheos was relatively higher than that of typical Pheos. Second, for a minority of the included MRI scans, DCE was not available, which is again imputable to the retrospective design; however, this issue did not impact the Pheo classification since the only typical Pheo without DCE showed all the remaining typical MRI features. Finally, histopathology was not available to confirm diagnosis in a few cases, but the high diagnostic accuracy of MIBG was deemed sufficient to serve as a reference standard for the purpose of this study [24].

In conclusion, the imaging characterization of typical Pheos may be performed using MRI with specific imaging

**Fig. 5** Atypical bilateral partially cystic Pheo with fat inclusions on ▶ the left side (#12, Table 2). Inhomogeneous round bilateral adrenal lesions, measuring each about 30 mm, are detected on T2-weighted MRI images (**A**, **B**); the right lesion had no change on T1-weighted out-of-phase, while the left lesion showed multiple foci of signal loss suggesting fat inclusion (**C**, **D**); both lesions showed inhomogeneous restricted diffusion (**E**, **F**) and enhancement on FS T1-weighted image (**G**, **H**)

features, but atypical Pheos represent a diagnostic challenge using MRI. For these tumors, a non-invasive accurate pre-operative diagnosis is required to avoid the use of biopsy and to plan the appropriate treatment strategy. For this purpose, MRI together with biochemical evaluation is recommended to characterize such adrenal tumors; however, cystic, necrotic, hemorrhagic, or fat changes may occur in atypical Pheos; thus, diagnostic pitfalls should be taken into consideration for imaging interpretation of such tumor type in clinical practice.

## Declarations

## References

1. Lattin GE, Sturgill ED, Tujo CA et al (2014) From the radiologic pathology archives: adrenal tumors and tumor-like conditions in the adult: radiologic-pathologic correlation. Radiographics 34:805–829. https://doi.org/10.1148/rg.343130127
2. Blake MA, Kalra MK, Maher MM et al (2004) Pheochromocytoma: an imaging chameleon. Radiographics 24:S87–S99. https://doi.org/10.1148/rg.24si045506
3. Lenders JWM, Duh Q-Y, Eisenhofer G et al (2014) Pheochromocytoma and paraganglioma: an endocrine society clinical practice guideline. j Clin Endocrinol Metab 99:1915–1942. https://doi.org/10.1210/jc.2014-1498
4. Romeo V, Maurea S, Guarino S et al (2018) The role of dynamic post-contrast T1-w MRI sequence to characterize lipid-rich and lipid-poor adrenal adenomas in comparison to non-adenoma lesions: preliminary results. Abdom Radiol 43:2119–2129. https://doi.org/10.1007/s00261-017-1429-4
5. Jacques AET, Sahdev A, Sandrasagara M et al (2008) Adrenal phaeochromocytoma: correlation of MRI appearances with histology and function. Eur Radiol 18:2885–2892. https://doi.org/10.1007/s00330-008-1073-z
6. Leung K, Stamm M, Raja A, Low G (2013) Pheochromocytoma: the range of appearances on ultrasound, CT, MRI, and functional imaging. Am J Roentgenol 200:370–378. https://doi.org/10.2214/AJR.12.9126
7. Raja A, Leung K, Stamm M et al (2013) Multimodality imaging findings of pheochromocytoma with associated clinical and biochemical features in 53 patients with histologically confirmed tumors. Am J Roentgenol 201:825–833. https://doi.org/10.2214/AJR.12.9576
8. Andreoni C, Krebs RK, Bruna PC et al (2008) Cystic phaeochromocytoma is a distinctive subgroup with special clinical, imaging and histological features that might mislead the diagnosis. BJU Int 101:345–350. https://doi.org/10.1111/j.1464-410X.2007.07370.x
9. Sahdev A (2017) Recommendations for the management of adrenal incidentalomas: what is pertinent for radiologists? Br J Radiol 90:20160627. https://doi.org/10.1259/bjr.20160627
10. Fassnacht M, Tsagarakis S, Terzolo M et al (2023) European Society of Endocrinology clinical practice guidelines on the management of adrenal incidentalomas, in collaboration with the European Network for the Study of Adrenal Tumors. Eur J Endocrinol 189:G1–G42. https://doi.org/10.1093/ejendo/lvad066
11. Maurea S, Klain M, Caracò C et al (2002) Diagnostic accuracy of radionuclide imaging using 131I nor-cholesterol or meta-iodobenzylguanidine in patients with hypersecreting or non-hypersecreting adrenal tumours. Nucl Med Commun 23:951–960. https://doi.org/10.1097/00006231-200210000-00004
12. Maurea S, Lastoria S, Caracò C et al (1996) The role of radiolabeled somatostatin analogs in adrenal imaging. Nucl Med Biol 23:677–680. https://doi.org/10.1016/0969-8051(96)00065-0
13. Lastoria S, Maurea S, Vergara E et al (1995) Comparison of labeled MIBG and somatostatin analogs in imaging neuroendocrine tumors. Q J Nucl Med 39:145–149
14. Araujo-Castro M, García Sanz I, Mínguez Ojeda C et al (2023) An integrated CT and MRI imaging model to differentiate between adrenal adenomas and pheochromocytomas. Cancers (Basel) 15:3736. https://doi.org/10.3390/cancers15143736
15. Varghese JC, Hahn PF, Papanicolaou N et al (1997) MR differentiation of phaeochromocytoma from other adrenal lesions based on qualitative analysis of T2 relaxation times. Clin Radiol 52:603–606. https://doi.org/10.1016/S0009-9260(97)80252-8
16. Barat M, Cottereau A-S, Gaujoux S et al (2022) Adrenal mass characterization in the era of quantitative imaging: state of the art. Cancers (Basel) 14:569. https://doi.org/10.3390/cancers14030569
17. Stanzione A, Romeo V, Maurea S (2023) The true value of quantitative imaging for adrenal mass characterization: reality or possibility? Cancers (Basel) 15:522. https://doi.org/10.3390/cancers15020522
18. Yi X, Guan X, Chen C et al (2018) Adrenal incidentaloma: machine learning-based quantitative texture analysis of unenhanced CT can effectively differentiate sPHEO from lipid-poor adrenal adenoma. J Cancer 9:3577–3582. https://doi.org/10.7150/jca.26356
19. Ansquer C, Drui D, Mirallié E et al (2020) Usefulness of FDG-PET/CT-based radiomics for the characterization and genetic orientation of pheochromocytomas before surgery. Cancers (Basel) 12:2424. https://doi.org/10.3390/cancers12092424
20. Gargan ML, Lee E, O'Sullivan M et al (2022) Imaging features of atypical adrenocortical adenomas: a radiological-pathological correlation. Br J Radiol. https://doi.org/10.1259/bjr.20210642
21. Nandra G, Duxbury O, Patel P et al (2020) Technical and interpretive pitfalls in adrenal imaging. Radiographics 40:1041–1060. https://doi.org/10.1148/rg.2020190080
22. Al Waeli DK, Albaghdadi FA, Naeem Mosa H (2023) Adrenal incidentaloma: a case report of pheochromocytoma (PCC) with atypical radiological features. JCEM Case Rep. https://doi.org/10.1210/jcemcr/luac014.005
23. Junejo SZ, Tuli S, Heimann DM et al (2017) A case report of cystic pheochromocytoma. Am J Case Rep 18:826–829. https://doi.org/10.12659/AJCR.905042
24. Garcia-Carbonero R, Matute Teresa F, Mercader-Cidoncha E et al (2021) Multidisciplinary practice guidelines for the diagnosis, genetic counseling and treatment of pheochromocytomas and paragangliomas. Clin Transl Oncol 23:1995–2019. https://doi.org/10.1007/s12094-021-02622-9